MOLECULAR AND CELLULAR BIOLOGY, Jan. 1997, p. 267–277 Vol. 17, No. 1
0270-7306/97/$04.00+0

Repair of Site-Specific Double-Strand Breaks in a Mammalian Chromosome by Homologous and Illegitimate Recombination

R. GEOFFREY SARGENT, MARK A. BRENNEMAN,† AND JOHN H. WILSON*

The Verna and Marrs McLean Department of Biochemistry, Baylor College of Medicine, Houston, Texas 77030

Received 15 July 1996/Returned for modification 31 August 1996/Accepted 3 October 1996

In mammalian cells, chromosomal double-strand breaks are efficiently repaired, yet little is known about the relative contributions of homologous recombination and illegitimate recombination in the repair process. In this study, we used a loss-of-function assay to assess the repair of double-strand breaks by homologous and illegitimate recombination. We have used a hamster cell line engineered by gene targeting to contain a tandem duplication of the native adenine phosphoribosyltransferase (APRT) gene with an I-*Sce*I recognition site in the otherwise wild-type APRT$^+$ copy of the gene. Site-specific double-strand breaks were induced by intracellular expression of I-*Sce*I, a rare-cutting endonuclease from the yeast *Saccharomyces cerevisiae*. I-*Sce*I cleavage stimulated homologous recombination about 100-fold; however, illegitimate recombination was stimulated more than 1,000-fold. These results suggest that illegitimate recombination is an important competing pathway with homologous recombination for chromosomal double-strand break repair in mammalian cells.

Chromosomal double-strand breaks are particularly dangerous lesions for cells; they can lead to the loss of chromosomes or chromosome segments or to the rearrangement of genetic information. Any of these outcomes is potentially lethal. To minimize these genetic consequences, most cells use two pathways for the repair of double-strand breaks: repair by homologous recombination and repair by illegitimate recombination. Whereas homologous recombination requires extensive tracts of sequence homology, illegitimate recombination is distinguished by its ability to join sequences with little or no homology.

The repair of double-strand breaks has been extensively studied in the yeast *Saccharomyces cerevisiae*, where chromosomal breaks induced in vivo are repaired almost exclusively by homologous recombination. Illegitimate recombination is observed only in cells defective in the Rad52 pathway or in cells where there is no homolog available for repair by homologous recombination (9, 18, 33). This is in contrast to mammalian cells, where the repair of double-strand breaks by illegitimate recombination occurs with high efficiency (27), often making it difficult to detect homologous recombination. Until recently, however, it has been difficult to study the repair of double-strand breaks at the molecular level in mammalian cells in a defined chromosomal context.

Induction of site-specific double-strand breaks has been demonstrated in mammalian and plant cells, as well as *S. cerevisiae*, by using the yeast intron-encoded I-*Sce*I and PI-*Sce*I endonucleases (3, 4, 10, 22, 24, 28). These enzymes have recognition sequences of 18 and 31 bp, respectively (5, 20), and should be found rarely, if at all, in mammalian genomes. Consistent with this expectation, expression of I-*Sce*I in mammalian cells appears to be nontoxic (28), and electroporation of PI-*Sce*I into human cells shows little cell killing (3). I-*Sce*I has been shown to stimulate recombination between extrachromosomal plasmids containing the I-*Sce*I recognition site (28, 31) and between extrachromosomal vectors and an I-*Sce*I-containing chromosomal target (4, 29). PI-*Sce*I has been shown to stimulate intrachromosomal homologous recombination between tandem repeats, one of which contained the PI-*Sce*I recognition site (3). These studies were designed as gain-of-function assays to study homologous recombination; however, illegitimate recombination events were also captured as unselected companion events (29) or as rare deletions that "corrected" insertion mutations (6).

The apparent stimulation of both homologous and illegitimate events led us to design a loss-of-function assay so that we could gauge the full spectrum of events stimulated by double-strand breaks. We used a tandem duplication of the adenine phosphoribosyltransferase (APRT) gene in CHO cells, in which the downstream copy was APRT$^+$ and wild type except for insertion of the I-*Sce*I recognition sequence in the second intron (Fig. 1). This modified APRT locus can become APRT$^-$ by homologous recombination (both crossovers and gene conversions), by illegitimate recombination (all forms of gene rearrangement [deletions, duplications, insertions, inversions, and translocations]), and by point mutation (base changes and frameshifts). These experiments show that both homologous and illegitimate recombination are substantially stimulated by I-*Sce*I-induced double-strand breaks.

MATERIALS AND METHODS

Vectors. The insertion vector, pGS90, used to create the GSAA5 cell line has the same structure as our previously described targeting vectors (30) except that an I-*Sce*I recognition sequence was introduced into the APRT intron 2 *Eco*RI site. To construct pGS90, a *Sal*I/*Not*I oligonucleotide was first cloned into the *Eco*RI site. This vector (pGS89) was then digested with *Sal*I and ligated to an oligonucleotide duplex containing the I-*Sce*I recognition site. The sequence of the I-*Sce*I modified site is shown in Fig. 7B.

The I-*Sce*I expression vector, pCMV-I-SceI, was kindly provided by Maria Jasin and contains the structural gene for the I-*Sce*I endonuclease driven by the cytomegalovirus (CMV) immediate-early gene enhancer/promoter, with a human growth hormone polyadenylation signal at the 3′ end (28). The transfection control vectors were pCMV-β-galactosidase (11), provided by Grant MacGregor, and pSXneoT_2AG_3, provided by Titia de Lange (8).

Cell construction. Targeted recombination with pGS90 was done as previously described (30) to modify the chromosomal hamster APRT gene and generate the recombination substrate shown in Fig. 1. One recombinant cell line (GSAA5) was identified, and its molecular structure was confirmed by Southern analysis and PCR. The cell line GS19-43 (Fig. 5), used to investigate the influence of double-strand breaks on illegitimate recombination, was isolated as a thymidine kinase-negative (TK$^-$) interval 1 crossover from GSAA5 cells.

* Corresponding author. Mailing address: Department of Biochemistry, Baylor College of Medicine, One Baylor Plaza, Houston, TX 77030. Phone: (713) 798-5760. Fax: (713) 796-9438. E-mail: jwilson@bcm.tmc.edu.

† Present address: Life Sciences Division, Los Alamos National Laboratory, Los Alamos, NM 87545.

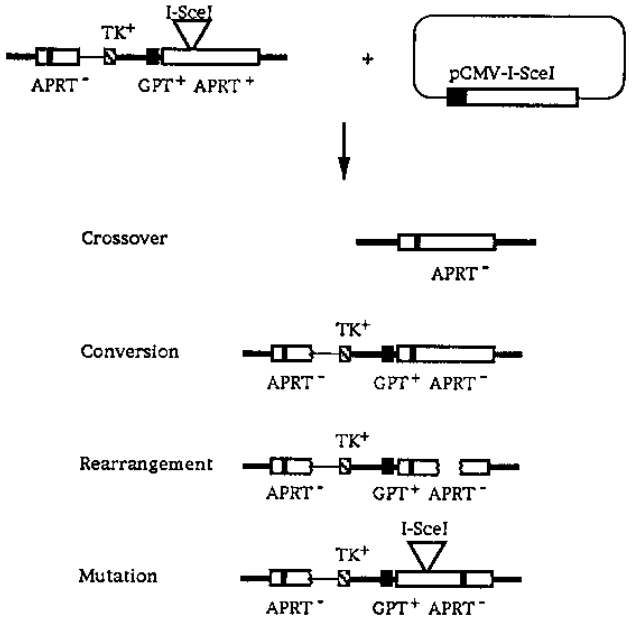

FIG. 1. I-*Sce*I-stimulated recombination products (not drawn to scale). For this and other figures, the thin line represents plasmid sequence and heavy lines represent chromosomal sequences. The APRT gene is schematically represented by an open box, the GPT gene is represented by a filled box, and the TK gene is represented by a cross-hatched box. The I-*Sce*I recognition sequence, located in intron 2, is represented by an inverted triangle. The heavy vertical line in the 5′ end of the chromosomal APRT$^-$ gene represents the exon 2 mutation that destroys the exon 2 *Eco*RV site; at other positions, it is used to represent undefined point mutations in the APRT gene. While the exon 2 *Eco*RV mutation alone is sufficient to render the cells APRT$^-$, the upstream copy of the APRT gene also has an engineered deletion encompassing a portion of exon 5 and the 3′ untranslated region (30).

Cell culture and recombination experiments. GSAA5 cells were transfected with uncut pCMV-I-SceI by calcium phosphate (14) or with the cationic lipid vesicle preparation Lipofectamine as recommended by the manufacturer (Gibco/BRL). After transfection, cells were grown for 5 to 7 days in nonselective medium to allow the expression of I-*Sce*I and the APRT$^-$ or TK$^-$ recombinant phenotypes. These cells were then harvested and replated in medium containing the drug fluoroiodoarabinosyluridine (FIAU) to select for TK$^-$ cells, in 8-aza-adenine to select for APRT$^-$ cells, or in medium containing both drugs to select for TK$^-$ APRT$^-$ cells (30). Cells were grown in selection for 2 weeks before drug-resistant colonies were picked and plates were stained for colony counts. To ensure that independent I-*Sce*I-induced events were characterized, only one colony was picked from an individual transfection for each drug selection and then expanded in nonselective medium for PCR and Southern analysis (30).

For illegitimate recombination experiments using GS19-43 cells, the same protocol was used except that selections were done in 8-aza-adenine to select for APRT$^-$ cells or 8-aza-adenine and 100 μM 6-thioguanine to select for APRT$^-$ guanine phosphoribosyltransferase-negative (GPT$^-$) cells. In transfections with the control vector pSXneoT$_2$AG$_3$, cells were replated 3 days after transfection at a density of 10^5 cells/100-mm-diameter dish into medium containing 375 μg of G418 per ml and grown in selection for 2 weeks before staining for colony counts. To assay for transfection efficiency, cells treated with the vector pCMV-β-galactosidase were replated 24 h after transfection and stained for β-galactosidase activity 48 h posttransfection (12).

DNA analysis. Southern analysis and PCR of the tandemly duplicated cell lines and their recombination products were done as previously described (30). The locations of PCR primers used for analysis of illegitimate recombinants are shown in Fig. 6, and their sequences are available on request. DNA sequencing was done on gel-purified PCR products, using a Stratagene Cycle Sequencing kit according to the manufacturer's instructions. Database searches of GenBank 89 were carried out by using the fastdb program in the IntelliGenetics suite.

RESULTS

Experimental design. To investigate the influence of double-strand breaks on intrachromosomal recombination, we used gene targeting to construct a 6.8-kb tandem duplication at the native APRT locus that contained an I-*Sce*I recognition site in intron 2 of the downstream copy of the APRT gene (Fig. 1). The structure of the recombination substrate in GSAA5 cells is analogous to those that we have used previously (30) and thus allows us to compare the effects of I-*Sce*I-induced cleavage with the effects of other modifications introduced at the same site in the APRT gene. The I-*Sce*I recognition site, which should be rare in the hamster genome, enables us to introduce a site-specific double-strand break in the APRT gene upon expression of I-*Sce*I endonuclease in cells transfected with pCMV-I-SceI (28).

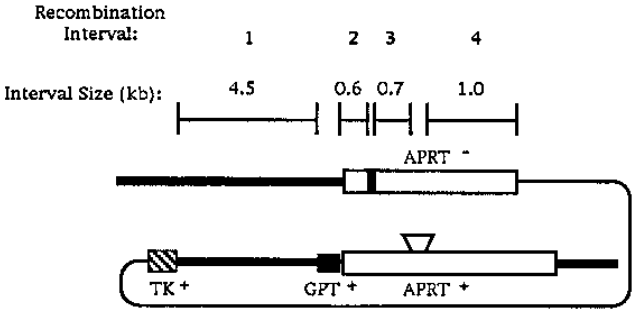

FIG. 2. Recombination intervals defined by sequence differences between the upstream and downstream copies of the APRT gene.

In these experiments, the I-*Sce*I expression vector, pCMV-I-SceI, was introduced into GSAA5 cells by treatment with calcium phosphate or cationic lipid vesicles. The effects of I-*Sce*I-generated double-strand breaks on recombination were assayed by plating cells in drug selection mixtures specific for the phenotypes of different recombinants, whose molecular structures were then determined by PCR and Southern analysis as previously described (30).

Since these cells are hemizygous for the APRT locus, homologous recombination in GSAA5 cells is limited to sequences shared by the tandem duplications. Similarly, in GS19-43 cells, which do not contain a tandemly duplicated structure (see Fig. 5), there is no chromosomal APRT copy for recombination repair.

Homologous recombination by crossovers. The tandem duplications in GSAA5 cells (Fig. 2) share 6.8 kb of homology that is divided into four intervals defined by three sequence differences between the upstream and downstream copies (the GPT gene, the exon 2 *Eco*RV site, and the intron 2 I-*Sce*I site). Crossovers, which eliminate one copy of the repeat and the intervening plasmid sequences, were selected in two ways: crossovers in any of the four intervals were selected as TK$^-$ cells by plating in FIAU; crossovers in intervals 3 and 4, which are TK$^-$ APRT$^-$, were selected by plating in FIAU and 8-aza-adenine.

Transfection of GSAA5 cells with the I-*Sce*I expression vector resulted in an 18- to 53-fold stimulation in the appearance of TK$^-$ cells and a 270- to 280-fold stimulation in TK$^-$ APRT$^-$ cells relative to transfection with pBluescript or pCMV-β-galactosidase (Table 1). On average, 2.9 cells per 10^4 cells surviving transfection have undergone a recombination event resulting in loss of the TK gene. No differences were observed between methods of transfection ($CaPO_4$ or Lipofectamine), nor was any stimulation of recombination observed in transfections with the control plasmids, pBluescript and pCMV-β-galactosidase.

If these I-*Sce*I-stimulated recombinants actually arose as a result of a double-strand break introduced at the I-*Sce*I site, then the distribution of crossover sites should be dramatically

TABLE 1. I-*Sce*I stimulation of chromosomal recombination

Expt	DNA	Treatment	Avg frequency[a] ± SD		
			TK^-	TK^- $APRT^-$	$APRT^-$
1	None	None	8 ± 4 (0.8)	0.2 ± 0.1 (0.2)	10 ± 13 (1.6)
	pBluescript	$CaPO_4$	11 ± 10 (1)	0.9 ± 0.7 (1)	6 ± 2 (1)
	pCMV-I-SceI	$CaPO_4$	580 ± 190 (53)	240 ± 24 (270)	1,200 ± 220 (200)
2	pBluescript + pCMV-β-galactosidase	Lipofectamine	13 ± 0.8 (1)	0.4 ± 0.1 (1)	22 ± 17 (1)
	pCMV-I-SceI + pCMV-β-galactosidase	Lipofectamine	230 ± 90 (18)	110 ± 20 (280)	1,600 ± 500 (73)

[a] Number of cells per 10^6 cells plated. Data for experiments 1 and 2 are from four independent transfections for each DNA. Fold stimulation relative to transfection by pBluescript or pBluescript plus pCMV-β-galactosidase for each transfection is indicated in parentheses.

different from that observed among spontaneous events: in contrast to spontaneous events, the majority of I-*Sce*I-stimulated events are expected to have a structure identical to that expected for a crossover in interval 4. (Because the I-*Sce*I site is expected to be eliminated by recombinational repair of the double-strand break, the actual crossover could have arisen in interval 3 or interval 4; we will refer to these products as interval 4 recombinants to emphasize the final structure.) The molecular structures of the APRT genes in several independent I-*Sce*I-stimulated TK^- and TK^- $APRT^-$ cells are summarized in Fig. 3A and compared to the distribution of spontaneously occurring TK^- and TK^- $APRT^-$ recombination products recovered in previous experiments (30). In pCMV-I-SceI transfections, 100% (11/11) of TK^- cells were interval 4 recombinants, in contrast to 15% (5/33) of spontaneous recombinants. Similarly, in pCMV-I-SceI transfections, 100% (12/12) of TK^- $APRT^-$ cells were interval 4 recombinants, compared to 54% (29/54) of spontaneous recombinants.

Homologous recombination by gene conversion. Gene conversions involve exchanges of sequence information between the repeats that do not alter the tandem structure. Here they are detected as a transfer of the *Eco*RV mutation from the upstream copy to the downstream copy, which yields $APRT^-$ cells that can be selected by plating in 8-aza-adenine. Among spontaneous events, gene conversions typically outnumber crossovers by 5 to 1 up to 10 to 1, accounting for about 80% of all events that lead to an $APRT^-$ phenotype (30).

Transfection of GSAA5 cells with the I-*Sce*I expression vector resulted in a 73- to 200-fold stimulation in the frequency of $APRT^-$ cells relative to transfection with pBluescript or pCMV-β-galactosidase (Table 1). On average, 1.4 cells per 10^3 cells surviving transfection have undergone a recombination event resulting in loss of APRT activity.

Analysis of the molecular structures of the APRT locus in 14 independent $APRT^-$ colonies revealed eight gene conversions, three crossovers, and three rearrangements (Fig. 3B). As with directly selected crossovers, the three crossovers recovered after selection for $APRT^-$ cells were interval 4 recombinants (data not shown).

If the gene conversion events arose as a result of a double-strand break introduced at the I-*Sce*I site, they are expected to have lost the I-*Sce*I site in addition to gaining the *Eco*RV mutation. As shown in Fig. 3B, 7 of 8 (88%) of the I-*Sce*I-stimulated convertants have lost the I-*Sce*I site, compared to 17 of 58 (30%) of spontaneous convertants. In addition, 6 of 8 (75%) of I-*Sce*I-stimulated convertants have coconverted the GPT gene, compared to 9 of 58 (16%) of spontaneous convertants. The single event that retained the I-*Sce*I site presumably represents a background spontaneous event.

In these experiments, $APRT^-$ cells can arise by mutation and rearrangements in addition to crossovers and gene conversion. In our analysis of spontaneous $APRT^-$ events 4 of 88 (5%) of $APRT^-$ cells arose by spontaneous point mutations but no rearrangements (0 of 88 $APRT^-$ cells) were detected (Fig. 3B). In pCMV-I-SceI-transfected cells, however, 3 of 14 (21%) of the $APRT^-$ cells resulted from a rearrangement that altered the structure of the locus (Fig. 3B). Southern analysis of these cell DNAs revealed that the upstream copy of the APRT gene was unaltered, as seen by the presence of a 6.0-kb *Bgl*II fragment in all three $APRT^-$ cell lines (Fig. 4A, lanes 2 to 4); however, the downstream copy was altered, as judged by the absence of the diagnostic 5.6-kb *Bgl*II fragment and the presence of novel fragments larger than the diagnostic fragment. PCR analysis showed that the downstream copy retained the GPT gene and the wild-type exon 2 *Eco*RV site (data not shown). The increased size of the *Bgl*II fragment coupled with the retention of sequences on both sides of the *Bgl*II site (the downstream *Bgl*II site is in an essential region; see Discussion) suggested that these rearrangements arose by insertion of DNA at the I-*Sce*I site. This was confirmed for GS20-5 and GS20-10, a cell line with a similar rearrangement that arose in a separate experiment, by DNA sequence analysis. The fine-structure analysis of these two insertions is shown in Fig. 7B.

Illegitimate recombination. The presence of three rearrangements among the 14 $APRT^-$ cells characterized above suggested that I-*Sce*I might stimulate illegitimate recombination in addition to homologous recombination. To investigate the influence of I-*Sce*I-induced double-strand breaks on illegitimate recombination, we used a cell line with a single wild-type copy of the APRT gene, which contained the I-*Sce*I recognition sequence in intron 2, and the upstream GPT gene (Fig. 5). This cell line, GS19-43, was isolated as an interval 1 crossover product from the GSAA5 cell line used in the experiments described above. In GS19-43 cells, $APRT^-$ point mutations and gene rearrangements can be selected with 8-aza-adenine, whereas GPT^- $APRT^-$ cells can be selected by using both 6-thioguanine and 8-aza-adenine.

Transfection of GS19-43 cells with the I-*Sce*I expression vector resulted in a 50- to 100-fold stimulation in the appearance of $APRT^-$ cells and a 55- to 85-fold stimulation in GPT^- $APRT^-$ cells relative to transfection with the control vector pCMV-β-galactosidase or $pSXneoT_2AG_3$ (Table 2). On average, about 3.8 cells per 10^4 of the pCMV-I-SceI cells surviving transfection underwent an event resulting in loss of APRT gene expression. Since the I-*Sce*I site is located in intron 2, 376 bp away from the nearest exon, certain types of rearrangements, small deletions in particular, will not be detected in these experiments. Thus, these measurements may underestimate the true frequency of I-*Sce*I-stimulated illegitimate recombination.

The molecular structures of these $APRT^-$ and $APRT^-$ GPT^- cells were determined by Southern analysis, PCR, and DNA sequencing. Two spontaneous $APRT^-$ cell DNAs, arising from control transfections, and 23 I-*Sce*I-stimulated $APRT^-$ and $APRT^-$ GPT^- cell DNAs were cut with *Bam*HI and analyzed by Southern blotting using the 4.0-kb *Bam*HI

A) Distribution of crossover recombinants.

Crossover Interval	Molecular Structure	TK⁻ Spontaneous	TK⁻ pCMV-I-SceI	TK⁻ APRT⁻ Spontaneous	TK⁻ APRT⁻ pCMV-I-SceI
1		23 (70%)	0	0	0
2		1 (3%)	0	0	0
3	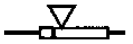	4 (12%)	0	25 (46%)	0
4	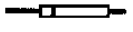	5 (15%)	11 (100%)	29 (54%)	12 (100%)
		33	11	54	12

B) Distribution of APRT⁻ recombinants.

	APRT⁻ Spontaneous	APRT⁻ pCMV-I-SceI
CROSSOVER 	11 (13%)	3 (21%)
CONVERSION 	73 (83%)	8 (58%)
REARRANGEMENT 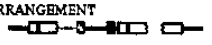	0	3 (21%)
MUTATION 	4 (5%)	0
	88	14

Gene Convertants	Spontaneous	pCMV-I-SceI
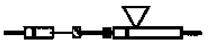	37 (64%)	1 (12.5%)
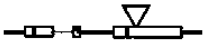	4 (7%)	0
	8 (14%)	1 (12.5%)
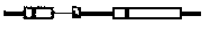	9 (16%)	6 (75%)
	58	8

FIG. 3. Distribution of recombinants. See Fig. 2 for a description of crossover intervals. Data for spontaneous recombination events are taken from a previous study of recombination in APRT, using similar tandemly duplicated structures (30).

APRT fragment as a hybridization probe (Fig. 4B). Unlike the two spontaneous mutants, which have retained the wild-type 4.0-kb fragment (Fig. 4B, lanes 4 and 5), DNAs from all 23 I-*Sce*I-stimulated APRT$^-$ or APRT$^-$ GPT$^-$ cells have lost the diagnostic 4.0-kb fragment and have acquired novel fragments. The gene rearrangements yielded either a single band (Fig. 4B, lanes 2, 3, and 6 through 16) or two bands (Fig. 4B, lanes 17 through 26).

To determine whether I-*Sce*I-stimulated rearrangements had altered the DNA sequence around the I-*Sce*I site, we used PCR analysis. Because amplification across the I-*Sce*I site was possible in only a minority of rearrangements (see below), we used PCR of sequences flanking the I-*Sce*I site (Fig. 6) to determine the extents of deleted DNA in these 23 APRT$^-$ cells and 12 additional I-*Sce*I-stimulated APRT$^-$ and APRT$^-$ GPT$^-$ cells. All 35 I-*Sce*I-stimulated APRT$^-$ cells retained sequences immediately downstream of the APRT gene, with the breakpoints mapping between position 3698 and the intron 2 I-*Sce*I site (Fig. 6). Of these 35 cell lines, 17 had deletions of less than 400 bp, and no cell lines that had deletions of greater than 8 kb were recovered.

Of the 11 I-*Sce*I-stimulated APRT$^-$ GPT$^-$ illegitimate recombinants isolated, seven cell lines had deletions of the GPT gene, as expected, whereas three lines retained a GPT gene indistinguishable by PCR from the wild-type GPT gene. Presumably these cells are GPT$^-$ due to point mutations or methylation of the GPT gene, but they have not been characterized further. Additionally, one I-*Sce*I-stimulated APRT$^-$ cell line gave a GPT$^-$ gene PCR product approximately 100 bp smaller than the wild-type GPT gene, presumably due to a small deletion within the gene.

DNA sequence analysis of gene rearrangements. Seven I-*Sce*I-stimulated gene rearrangements, five from experiments using GS19-43 cells and two from experiments using GSAA5

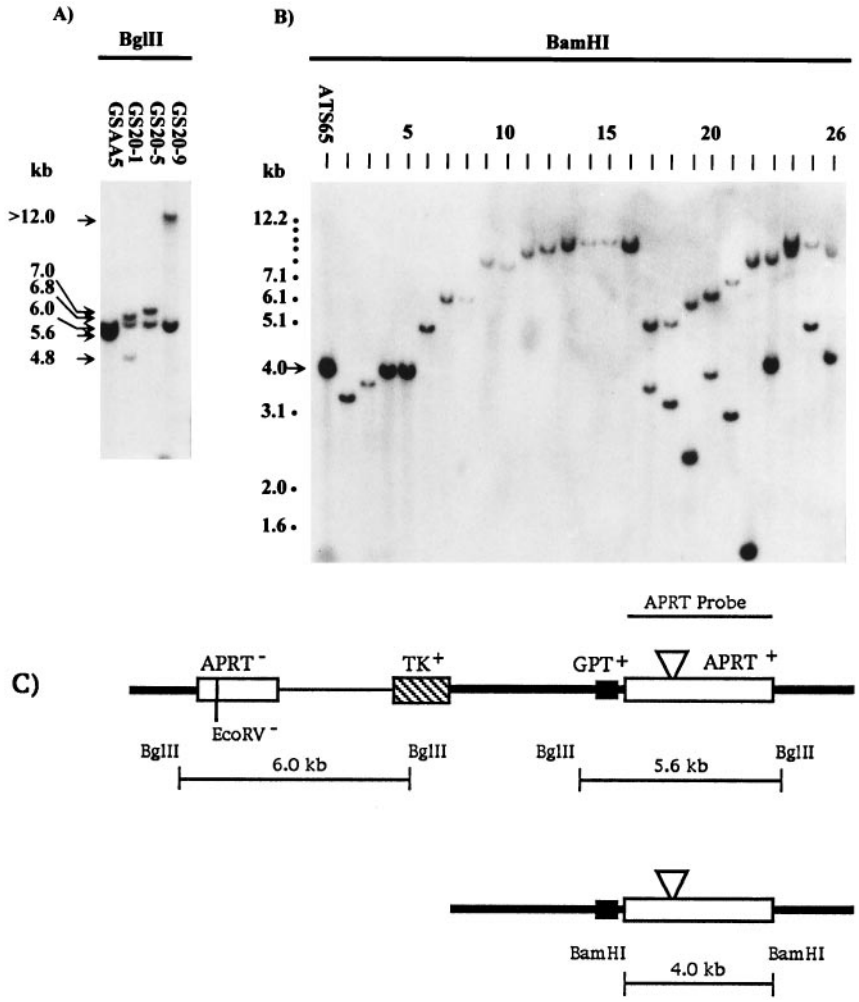

FIG. 4. Southern analysis of gene rearrangements recovered from pCMV-I-SceI transfections of GSAA5 and GS19-43 cells. Genomic DNAs from I-*Sce*I-stimulated APRT$^-$ GSAA5 cells that were identified as gene rearrangements, or from the parental GSAA5 cell line, were digested by *Bgl*II (A), or DNAs from I-*Sce*I-stimulated APRT$^-$ or APRT$^-$ GPT$^-$ GS19-43 cells were digested by *Bam*HI (B). For panel B, DNA from ATS65 cells (lane 1), which have a full-length 4.0-kb APRT gene containing the exon 2 *Eco*RV mutation, was included as a wild-type APRT size marker; also included was DNA from two spontaneously arising APRT$^-$ cells recovered from transfections with pBluescript + pCMV-β-galactosidase (lanes 4 and 5). In panel A, the fragment sizes are indicated by arrows; in panel B, the full-length 4.0-kb APRT *Bam*HI fragment is indicated by an arrow, and positions of 1-kb ladder markers (Gibco/BRL) are indicated by bullets. The restriction sites and their predicted products are shown in panel C. The APRT 4.0-kb *Bam*HI fragment was used as a probe for panels A and B.

cells (cell lines GS20-5 and GS20-10), were amplifiable by PCR primers that spanned the rearrangements. The lack of PCR amplification for other rearrangements may indicate that they arose by translocation, inversion, or insertion of a large segment of DNA. We have not characterized these rearrangements further. The structures of the amplifiable rearrangements were examined by DNA sequencing. A fine-structure map and the DNA sequences across the rearrangement junctions are shown in Fig. 7.

Six of seven of the PCR-amplified gene rearrangements have rearrangement junctions in the I-*Sce*I recognition sequence. The sole exception, rearrangement 1 (Fig. 7), has an intact I-*Sce*I site with a deletion between APRT nucleotides 1592 and 1773; this event may have arisen spontaneously. Rearrangements 2 and 3 (Fig. 7) are 529- and 826-bp deletions, respectively, both with one junction in the I-*Sce*I recognition sequence. All three deletions cover exon sequences, which is sufficient to account for their APRT$^-$ phenotypes.

Rearrangements 4 through 7 have novel DNA sequences inserted into the I-*Sce*I recognition site ranging in size from approximately 0.9 to 2.1 kb. Only rearrangement 7 had a substantial accompanying deletion of 866 bp extending into exon 2; the other three rearrangements retained sequences from both halves of the I-*Sce*I recognition site. In rearrangement 6, the single-strand extensions left by I-*Sce*I cleavage were both retained in the product (boldface TTAT in Fig. 7).

Two of the insertions originated from vector DNA used in the transfections (rearrangements 6 and 7). In rearrangement 6, part of the CMV enhancer/promoter, used to drive the I-*Sce*I and β-galactosidase genes, was linked to the 5′ half of the I-*Sce*I recognition site, while noncontiguous plasmid sequence encoding the β-galactosidase gene was linked to the 3′ half of the I-*Sce*I site. In rearrangement 7, an unidentified DNA sequence was linked to the junction in exon 2, whereas part of the CMV enhancer/promoter was linked to the 3′ half of the I-*Sce*I site.

The remaining two insertions originated from chromosomal locations outside the APRT locus. In rearrangement 4, an unidentified DNA sequence was linked to the 5′ half of the I-*Sce*I sequence, and insert DNA with 80% identity to a human

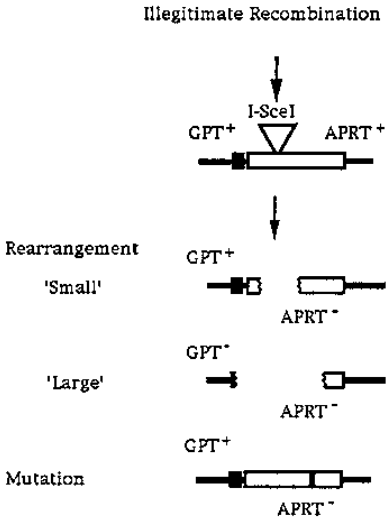

FIG. 5. The APRT locus in GS19-43 cells along with potential rearrangements and point mutations.

Alu repeat (17) was linked to the 3′ half of the I-*Sce*I site. Presumably this repeat has been conserved between hamster and human cells. The 5′ side of the rearrangement 5 insert had an unusual conversion of I-*Sce*I sequence to wild-type APRT sequence with a duplication of at least 58 bp of downstream APRT sequence. The extent of this duplication has not been determined. The insert DNA at the 3′ side of the rearrangement shows 60% identity to an L1 repeat (34).

The characteristics of the junctions described here are typical of illegitimate recombination junctions generated by the joining of DNA ends seen in other studies (6, 10, 15, 21, 27, 25, 29). Of the six junctions where the recombining DNAs are known, rearrangements 2 and 6 had no homology at the junctions, three rearrangements had microhomologies at the junction (rearrangements 1 and 3 had one nucleotide of homology, and rearrangement 7 had three nucleotides of homology), and one (rearrangement 6) had a 2-bp insert.

DISCUSSION

Using loss-of-function assays at the APRT locus in CHO cells, we have shown that I-*Sce*I-induced site-specific double-strand breaks substantially stimulate both homologous recombination and illegitimate recombination in mammalian cells. Homologous recombination was assayed in a targeted cell line that carried a 6.8-kb duplication of the APRT gene and 5′ flanking sequences (Fig. 2). Expression of I-*Sce*I endonuclease from a transfected vector stimulated crossover recombination 20- to 50-fold over the entire 6.9 kb of homology (TK^- selection [Table 1]) and 270- to 280-fold in a narrower 1.7-kb segment of the APRT gene (TK^- $APRT^-$ selection [Table 1]). Previously we had used a gain-of-function assay at the hypoxanthine/guanine phosphoribosyltransferase locus in human cells to demonstrate that site-specific double-strand breaks, which were generated by electroporation of PI-*Sce*I endonuclease, stimulated homologous crossover recombination in a 6.9-kb interval in a dose-dependent manner, up to a maximum of 10-fold after treatment with 500 U of enzyme (3). The greater stimulation of crossover recombination observed in the present studies is likely due to increased levels, or greater persistence, of expressed I-*Sce*I compared to electroporated PI-*Sce*I but could also be due to a difference in the efficiency of cleavage in the two assay systems.

TABLE 2. I-*Sce*I stimulation of illegitimate recombination after Lipofectamine treatment

DNA	Avg frequency[a] ± SD	
	$APRT^-$	$APRT^-$ GPT^-
$pSXneoT_2AG_3$ + pCMV-β-galactosidase	5 ± 2 (1)	2 ± 0.8 (1)
pCMV-I-SceI + pCMV-β-galactosidase	250 ± 40 (50)	110 ± 11 (55)
pCMV-I-SceI + $pSXneoT_2AG_3$	500 ± 40 (100)	170 ± 29 (85)

[a] Number of cells per 10^6 cells plated. The data represent six independent transfections for each DNA. Fold stimulation relative to transfection by $pSXneoT_2AG_3$ plus pCMV-β-galactosidase is indicated in parentheses.

In our previous studies with PI-*Sce*I, we were unable to determine whether crossovers were stimulated at the site of the suspected break because the 6.9-kb duplicated segments were identical except for the PI-*Sce*I recognition site. In this study, the duplicated region was divided into four intervals by sequence differences between the upstream and downstream copies of the APRT gene (Fig. 2), allowing us to determine whether the stimulated events were generated by crossovers near the I-*Sce*I recognition site. All 26 crossover recombinants that were analyzed (Fig. 3) were interval 4 recombinants, as expected if the recombination events were initiated by a double-strand break at the I-*Sce*I recognition site. This distribution of recombinants is dramatically different from that observed for spontaneous events, which were distributed in intervals of homology in proportion to the relative length of the interval (Fig. 3).

Among spontaneous homologous recombinants at the APRT locus, gene conversions outnumber crossovers by 6- to 10-fold (Table 3). Among I-*Sce*I-stimulated events, gene conversions are also more numerous than crossovers, but only by about three- to fivefold, as assessed by frequency (8.4×10^{-4} versus 1.8×10^{-4} [Table 3]) and by distribution of events (8 versus 3 Fig. 3B). Analysis of individual convertants showed that seven of eight had coconverted the I-*Sce*I recognition site and the *Eco*RV site, as expected if the events were initiated by breaks at the I-*Sce*I site and were converted to an $APRT^-$ phenotype by transfer of the *Eco*RV mutation from the upstream copy (Fig. 3B). Of these seven events, six had also converted the GPT gene, which is 0.6 kb upstream of the *Eco*RV site (Fig. 3B). Among comparable spontaneous events, only 9 of 17 had coconverted the GPT gene (Fig. 3B). We explore this difference in more detail below.

By using a loss-of-function assay at the APRT locus in GSAA5 cells, which contain the tandem duplication of APRT sequences, we were able to compare homologous recombination (conversions and crossovers), illegitimate recombination (rearrangements), and point mutation. Of 14 I-*Sce*I-stimulated events, 11 arose by homologous recombination, 3 were found to have rearrangements in the downstream copy of the APRT gene, and none were identified as point mutants (Fig. 3B). (In this study, point mutants are operationally defined: they possess the same tandemly duplicated structure as the parent, as assessed by Southern blotting and PCR; however, they lack the *Eco*RV mutation in the downstream copy, which distinguishes them from gene convertants.) The >10-fold change in the ratio of rearrangements recovered from spontaneous $APRT^-$ versus I-*Sce*I-treated cells (0/88 versus 3/14) coupled with the 100-fold change in the frequency of $APRT^-$ cells (Table 1) suggests that I-*Sce*I cleavage stimulates illegitimate recombination more than 1,000-fold.

We confirmed this high-level of stimulation by using

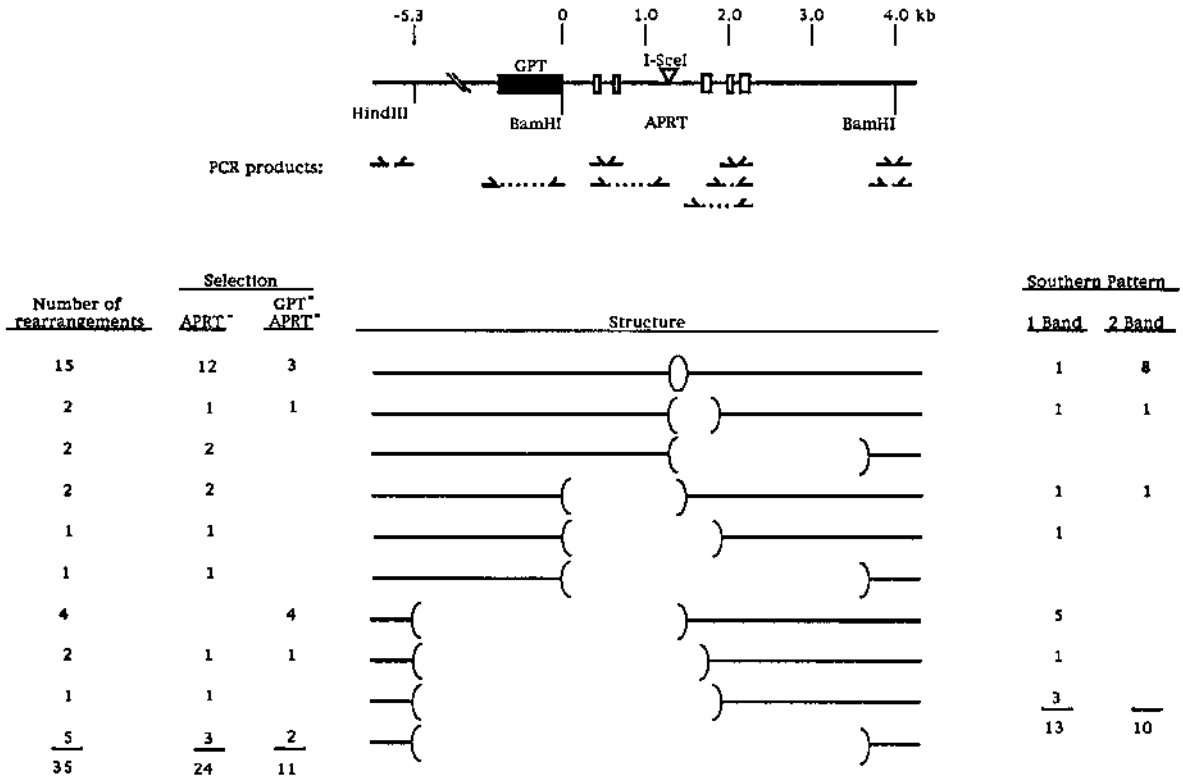

FIG. 6. PCR analysis of flanking sequences from I-*Sce*I-transfected GS19-43 APRT$^-$ and GPT$^-$ APRT$^-$ gene rearrangements. A total of 35 APRT$^-$ and GPT$^-$ APRT$^-$ cell lines were analyzed by PCR; 23 of the 35 were also characterized by Southern analysis (Fig. 4B). In this figure and Fig. 7, the five APRT exons are indicated as open boxes. Numbering is relative to the *Bam*HI site 5′ of the APRT locus, which is designated position 0. The brackets at the ends of the heavy lines represent the nearest flanking PCR primer to the intron 2 I-*Sce*I site that yields a PCR product; thus, the bracketed regions indicate the maximum possible size of deletions.

GS19-43 cells, which contain a single copy of the APRT gene (Fig. 5), to examine the effects of I-*Sce*I expression on illegitimate recombination in the absence of homologous recombination. Treatment of these cells with I-*Sce*I increased the frequency of APRT$^-$ cells 50- to 100-fold over spontaneous levels (Table 2). Analysis of 35 independent I-*Sce*I-stimulated events showed that all 35 carried identifiable rearrangements. By contrast, analysis of eight independent spontaneous events that arose in control transfections with pSXneoT$_2$AG$_3$ and pCMV-β-galactosidase showed that all eight resulted from point mutation. This limited analysis of spontaneous events is consistent with previous studies (16, 19), which showed that about 1 in 10 spontaneous APRT$^-$ cells carries a rearrangement. Once again, the change in the ratio of rearrangements to point mutations (0/8 to 35/35) coupled with the change in frequency of APRT$^-$ cells suggests that I-*Sce*I cleavage stimulates illegitimate recombination more than 1,000-fold.

The observation that double-strand breaks stimulate illegitimate recombination more than homologous recombination (~1,000-fold versus ~100-fold) suggests that mammalian cells may preferentially repair double-strand breaks by illegitimate recombination, as has been suggested previously (26, 27). This is almost certainly the case in the G$_1$ phase of the cell cycle because interchromosomal homologous recombination is exceedingly rare in mammalian somatic cells, even after a double-strand break is introduced (1a, 6). In the rest of the cell cycle, homologous repair of a break could occur by using the sister chromatid as the intact template. From genetic studies of mouse cells, using tandem duplications analogous to the one used here, it has been estimated that 80% of spontaneous homologous recombination events occur between the upstream and downstream copies on sister chromatids (2). What is unknown is the frequency with which homologous recombination involves the identical copy on the sister chromatid; such an event occurs without genetic consequence in somatic cells and thus would remain undetected in genetic experiments. Until the magnitude of this class of events is defined, it is not possible to draw firm conclusions about the relative contributions of homologous and illegitimate recombination to the repair of double-strand breaks.

Of the 35 I-*Sce*I-stimulated rearrangements that were characterized, 34 had alterations affecting the I-*Sce*I site, as expected if a double-strand break were introduced at that point. PCR analysis was used to estimate the extent of DNA lost from the broken ends (Fig. 6). More than half of the ends retained DNA identified by the PCR primers closest to the I-*Sce*I recognition site: 19 of 34 left ends retained DNA within 34 nucleotides of the cut site; 21 of 34 right ends retained DNA within 20 nucleotides of the cut site. None of the right ends had lost DNA identified by a primer at position 3698, which is within the putative final exon for a convergently transcribed essential gene (1, 8a, 15). Since these cells are hemizygous for the region around the APRT gene and thus have a single copy of this essential gene, loss of this DNA would be lethal. Although the presence of an essential gene limits the loss of DNA that can be observed downstream of the APRT gene, it is useful in studying rearrangements involving the APRT locus since it provides a preserved sequence tag adjacent to the site of rearrangement. Loss of DNA from the left ends is unrestricted by essential sequences for at least 170 kb on the 5′ side

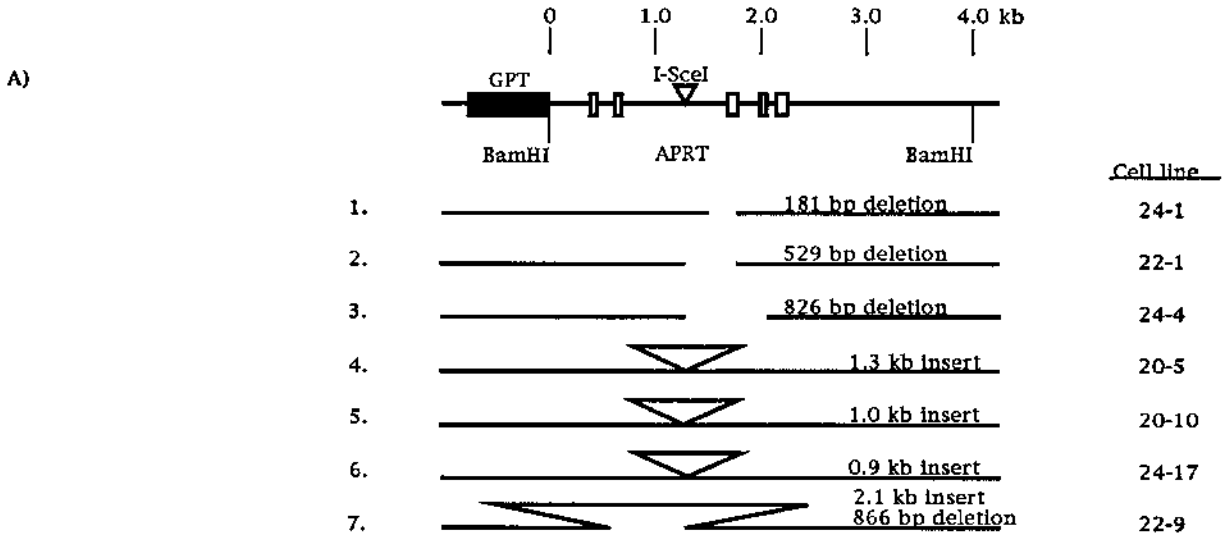

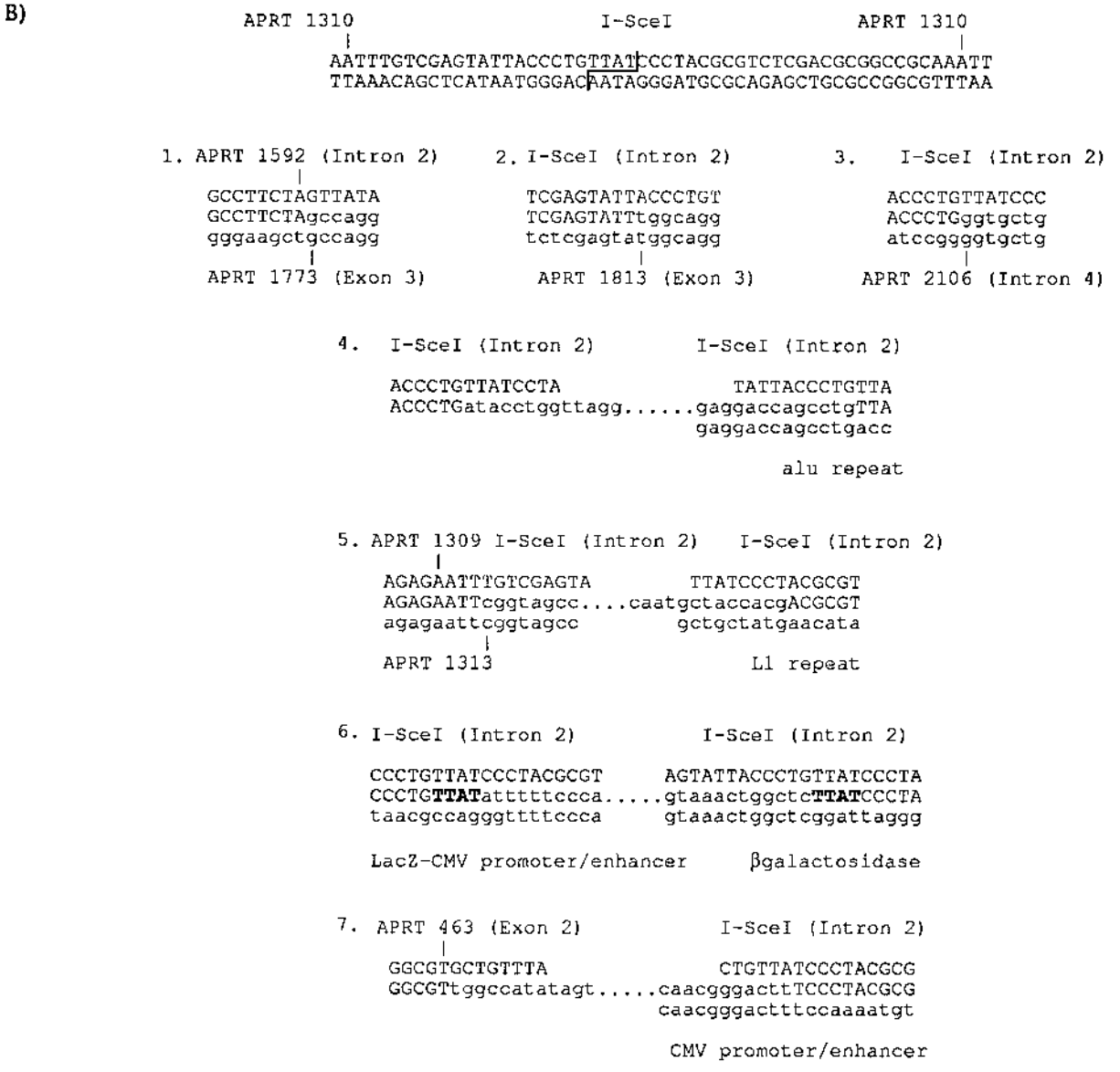

TABLE 3. Relative contributions of the genetic processes that generate the spectrum of APRT$^-$ cells that arise spontaneously and after I-*Sce*I treatment

Genetic process	Spontaneous			I-*Sce*I stimulated			Frequency/rate[e]
	Rate[a] (10^{-8})	Distribution[b]		Frequency[c] (10^{-5})	Distribution[d]		
		Tandem	Single		Tandem	Single	
Conversion	124	73		84	8		680
Crossover	12	11		18	3		1,500
Rearrangement	1	0	0	38	3	35	38,000
Mutation	10	4	8	≤1	0	0	≤100
Total		88	8		14	35	

[a] Calculated from data of Nalbantoglu et al. (19), Meuth et al. (16), and Sargent et al. (30). The rate for crossover is an average of TK$^-$ APRT$^-$ rate measurements made on three cell lines with duplicated APRT sequences identical to those in this study except for the specific DNA at the site of the I-*Sce*I recognition sequence (30). The rates for mutation and rearrangement were made in cells with a single wild-type copy of APRT (19, 16), similar to GS19-43 cells; the overall rate at which APRT$^-$ cells were generated was apportioned into a mutation rate and a rearrangement rate based on the distribution into those two classes of independent events isolated in that study. The rate of conversion was calculated as the overall rate at which APRT$^-$ cells were generated (1.47×10^{-6}) in the three cell lines with duplicated APRT sequences used by Sargent et al. (30) minus the calculated rates for conversion, rearrangement, and mutation.

[b] The left column shows the distribution of spontaneous events that led to APRT$^-$ cells in cell lines that carry tandem duplications analogous to the one used in these studies (30). The right column shows the distribution of spontaneous events that led to APRT$^-$ cells in cell line GS19-43, which carries a single copy of APRT.

[c] The frequency of I-*Sce*I-stimulated TK$^-$ APRT$^-$ crossovers is averaged from experiments 1 and 2 in Table 1. The frequency of I-*Sce*I-stimulated APRT$^-$ rearrangements is taken as the average frequency of APRT$^-$ cells observed after I-*Sce*I treatment of cell line GS19-43 (Table 2), since no mutants were found among 35 events analyzed. The frequency of I-*Sce*I-stimulated point mutations is estimated to be 10^{-5} or less, based on the average frequency of APRT$^-$ cells (3.8×10^{-4}) observed after I-*Sce*I treatment of cell line GS19-43 and the absence of point mutants among 35 events analyzed (Table 2). The frequency of I-*Sce*I-stimulated conversions is the average frequency of APRT$^-$ cells observed after I-*Sce*I treatment of cell line GSAA5 (1.40×10^{-3}; Table 1) minus the frequencies of crossovers and rearrangements.

[d] The left column shows the distribution of I-*Sce*I-stimulated events that led to APRT$^-$ cells in cell line GSAA5, which carries tandemly duplicated APRT sequences (Fig. 3A). The right column shows the distribution of I-*Sce*I-stimulated events that led to APRT$^-$ cells in cell line GS19-43, which carries a single copy of APRT.

[e] Ratio of I-*Sce*I-stimulated frequencies to spontaneous rates, calculated to give a measure of the relative effects of I-*Sce*I treatment on conversion, crossover, rearrangement, and mutation. Because frequencies and rates cannot be compared directly, the ratio is not a measure of the fold stimulation.

of the APRT gene (16); hence, the observed loss (Fig. 6) probably reflects the natural extent of cellular processing of the I-*Sce*I-induced double-strand breaks. Losses of greater than 8 kb were not observed among the analyzed rearrangements. Furthermore, since all of the rearrangements with the two-band Southern pattern (Fig. 4B, lanes 17 to 26) retained both *Bam*HI sites by PCR analysis (Fig. 6), these rearrangements could be explained as translocations, inversions, or large insertions (in some cases of up to 18 kb).

The analysis of I-*Sce*I-induced rearrangements at the DNA sequence level was identified by sequencing PCR products for five rearrangements isolated from GS19-43 cells and for two rearrangements isolated from GSAA5 cells (Fig. 7). (The rest of the rearrangements failed to amplify by PCR, as might be expected for translocations, inversions, or large insertions.) The characterized rearrangements included three deletions and four insertions. The inserted DNAs, which were partially sequenced, included plasmid sequences attached to three of the eight ends and presumptive chromosomal sequences attached to five of the eight ends. All three deletions and one of the insertions had lost at least one APRT exon, which accounted for their APRT$^-$ phenotype. Three of the insertions had not deleted essential APRT sequences yet were also APRT$^-$; presumably they are APRT$^-$ either because their inserted DNAs interfere with APRT expression (23) or because they suffered associated mutations in essential APRT sequences. The latter possibility could explain the four rearrangements that were isolated by selection for GPT$^-$ APRT$^-$ cells yet retained GPT sequences (Fig. 6); by PCR, one of these rearrangements has a GPT gene that is about 100 bp shorter than normal. Additional examples of this category are being isolated for sequence analysis of the GPT gene to determine whether illegitimate repair of double-strand breaks is associated with collateral mutations, as has been observed for homologous repair of double-strand breaks in *S. cerevisiae* (32).

The spectrum of rearrangements observed here differs from that observed for rearrangements induced at the APRT locus by electroporation of restriction enzymes (21), presumably due to differences in experimental design. In those experiments, the electroporated restriction endonucleases cut in APRT exons and the majority of induced rearrangements were small deletions (of 1 to 36 bp) and insertions (of 1 to 273 bp); only 13 of 127 APRT$^-$ mutants were the result of larger rearrangements (21). In our experiments, the I-*Sce*I site is in intron 2, 376 bp away from the closest exon; thus, small deletions, for example, are not adequate to generate an APRT$^-$ phenotype. The absence of this prominent class of small rearrangements in our experiments suggests that we may significantly underestimate the stimulation of illegitimate recombination by I-*Sce*I cleavage.

How insertions and more complex rearrangements arise is unclear. They could arise by joining of DNA ends: insertions by the capture of DNA fragments as is likely the case for plasmid inserts (Fig. 7) or complex rearrangements by joining with other chromosome breaks. Alternatively, or in addition, they could arise by the copy-join process recently proposed as a mechanism for random integration (13). According to this mechanism, the exposed I-*Sce*I-cut ends would invade extra-

FIG. 7. Fine-structure analysis and DNA sequences of gene rearrangements recovered from I-*Sce*I-treated cells. The heavy lines in panel A represent remaining APRT sequences and inserted DNA sequences. The sequence of the polylinker and I-*Sce*I sequence in GSAA5 and GS19-43 cells are shown in panel B with the 4-bp TTAT 3′ overhang generated by I-*Sce*I cleavage. In the sequence alignments, the top strand (uppercase) represents APRT gene sequence, the middle sequence in (upper- and lowercase) represents the junction sequences, and the bottom sequence (lowercase) represents sequence from inserted DNAs, where the source of inserted DNA is known or suspected. Duplicated sequences at the rearrangement junctions are indicated in boldtype. Only those sequences that were identified in GenBank 89 database searches are indicated.

chromosomal or chromosomal DNA and prime DNA synthesis, linking the I-*Sce*I ends to new DNA sequences. Depending on the site, or sites, of invasion, this could lead to inversions, duplications, or translocations. On the other hand, if the invading strand and newly copied DNAs were released and joined to the other I-*Sce*I end, an insertion would be generated. In principle, multiple cycles of invasion, copying, and release could generate complex insertions that are derived from several genomic locations.

Overall, this study has investigated the relative contributions of homologous recombination (conversion and crossover), illegitimate recombination (rearrangement), and point mutation to the production of APRT$^-$ cells after treatment with I-*Sce*I endonuclease (Table 3). As summarized above, homologous recombination was stimulated at least 100-fold relative to spontaneous events, illegitimate recombination was stimulated at least 1,000-fold, and point mutations (unassociated with rearrangements) were stimulated 10-fold or less. The same rank order is evident in a comparison of the frequencies of I-*Sce*I-stimulated events determined in this study with the previously published rates of spontaneous events (16, 30): illegitimate recombination (rearrangement) was stimulated ~10-fold more than homologous recombination (conversion plus crossover) and at least 100-fold more than point mutations (Table 3).

The molecular events responsible for initiating spontaneous homologous recombination between chromosomal sequences in somatic cells are undefined. There is growing evidence that in *S. cerevisiae*, the initiating events during meiotic recombination are double-strand breaks (7, 35). Is it possible that the initiating events for spontaneous homologous recombination in somatic cells are also double-strand breaks? Analysis of I-*Sce*I-induced double-strand breaks at the APRT locus suggests that the answer may be no. If spontaneous double-strand breaks behaved like I-*Sce*I-induced breaks, then spontaneous rearrangements would be expected to occur at about the same level as spontaneous conversions and crossovers, but they do not (Table 3). It may be, however, that I-*Sce*I-induced breaks differ significantly from spontaneous breaks in location, nature of the cleaved ends, or I-*Sce*I binding at the ends (20). Whatever events initiate spontaneous homologous recombination, they only rarely lead to rearrangements.

ACKNOWLEDGMENTS

We thank the members of the Wilson laboratory for their criticisms and encouragement. We greatly appreciate PCR primers supplied by Gerry Adair and the plasmids supplied by Maria Jasin, Titia de Lange, and Grant MacGregor.

This investigation was supported by NIH grant GM38219 to J.H.W. and NRSA GM14594 to R.G.S.

REFERENCES

1. **Adair, G.** Personal communication.
1a. **Benjamin, M. B., and J. B. Little.** 1992. X rays induce interallelic homologous recombination at the human thymidine kinase gene. Mol. Cell. Biol. **12:**2730–2738.
2. **Bollag, R. J., and R. M. Liskay.** 1991. Direct-repeat analysis of chromatid interactions during intrachromosomal recombination in mouse cells. Mol. Cell. Biol. **11:**4839–4845.
3. **Brenneman, M., F. S. Gimble, and J. H. Wilson.** 1996. Stimulation of intrachromosomal homologous recombination in human cells by electroporation with site-specific endonucleases. Proc. Natl. Acad. Sci. USA **93:**3608–3612.
4. **Choulika, A., A. Perrin, B. Dujon, and J.-F. Nicolas.** 1995. Induction of homologous recombination in mammalian chromosomes by using the I-*Sce*I system of *Saccharomyces cerevisiae*. Mol. Cell. Biol. **15:**1968–1973.
5. **Gimble, F. S., and J. Wang.** 1996. Substrate recognition and induced DNA distortion by the PI-SceI endonuclease, an enzyme generated by protein splicing. J. Mol. Biol. **263:**163–180.
6. **Godwin, A. R., R. J. Bollag, D. M. Christie, and R. M. Liskay.** 1994. Spontaneous and restriction enzyme-induced chromosomal recombination in mammalian cells. Proc. Natl. Acad. Sci. USA **91:**12554–12558.
7. **Haber, J. E.** 1992. Exploring the pathways of homologous recombination. Curr. Opin. Cell Biol. **4:**401–402.
8. **Hanish, J. P., J. L. Yanowitz, and T. de Lange.** 1994. Stringent requirements for the formation of human telomeres. Proc. Natl. Acad. Sci. USA **91:**8861–8865.
8a. **Harwood, J., and M. Meuth.** 1995. Deletion mapping of highly conserved transcribed sequence downstream from APRT locus. Somatic Cell Mol. Genet. **21:**151–160.
9. **Kramer, K., J. A. Brock, K. Bloom, J. K. Moore, and J. E. Haber.** 1994. Two different types of double-strand breaks in *Saccharomyces cerevisiae* are repaired by similar Rad52-independent, nonhomologous recombination events. Mol. Cell. Biol. **14:**1293–1301.
10. **Lukacsovich, T., D. Yang, and A. S. Waldman.** 1994. Repair of a specific double-strand break generated within a mammalian chromosome by yeast endonuclease I-SceI. Nucleic Acids Res. **22:**5649–5657.
11. **MacGregor, G. R., and C. T. Caskey.** 1989. Construction of plasmids that express *E. coli* β-galactosidase in mammalian cells. Nucleic Acids Res. **17:**2365.
12. **MacGregor, G. R., G. P. Nolan, S. Fiering, M. Roederer, and L. A. Herzenberg.** 1989. Use of *E. coli lacZ* (β-galactosidase) as a reporter gene, p. 1–19. *In* E. J. Murray and J. M. Walker (ed.), Gene expression *in vivo*. Humana Press, Clifton, N.J.
13. **Merrihew, R. V., K. Marburger, S. L. Pennington, D. B. Roth, and J. H. Wilson.** 1996. High-frequency illegitimate integration of transfected DNA at preintegrated target sites in a mammalian genome. Mol. Cell. Biol. **16:**10–18.
14. **Merrihew, R. V., R. G. Sargent, and J. H. Wilson.** 1995. Efficient modification of the APRT gene by FLP/FRT site-specific targeting. Somatic Cell Mol. Genet. **21:**299–307.
15. **Meuth, M.** 1989. Illegitimate recombination in mammalian cells, p. 833–860. *In* D. E. Berg and M. M. Howe (ed.), Mobile DNA. American Society for Microbiology, Washington, D.C.
16. **Meuth, M., C. Miles, G. Phear, and G. Sargent.** 1990. Molecular patterns of APRT gene rearrangements, p. 305–314. *In* M. L. Mendelshon and R. J. Albertini (ed.), Mutation and the environment. Wiley-Liss, New, N.Y.
17. **Meyers, J. C., et al.** 1983. Analysis of the 3′ end of the human pro-alpha 2(I) collagen gene. Utilization of multiple polyadenylation sites in cultured fibroblasts. J. Biol. Chem. **258:**10128–10135.
18. **Moore, J. K., and J. E. Haber.** 1996. Cell cycle and genetic requirements of two pathways of nonhomologous end-joining repair of double-strand breaks in *Saccharomyces cerevisiae*. Mol. Cell. Biol. **16:**2164–2173.
19. **Nalbantoglu, J., O. Goncalves, and M. Meuth.** 1983. Structure of mutant alleles at the *aprt* locus of Chinese hamster ovary cells. J. Mol. Biol. **167:**575–594.
20. **Perrin, A., M. Buckle, and B. Dujon.** 1993. Asymmetrical recognition and activity of the I-SceI endunuclease in its site and on intron-exon junctions. EMBO J. **12:**2939–2947.
21. **Phillips, J. W., and W. F. Morgan.** 1994. Illegitimate recombination induced by DNA double-strand breaks in a mammalian chromosome. Mol. Cell. Biol. **14:**5794–5803.
22. **Plessis, A., A. Perrin, J. Haber, and B. Dujon.** 1992. Site-specific recombination determined by I-SceI, a mitochondrial group I intron-encoded endonuclease expressed in the yeast nucleus. Genetics **130:**451–460.
23. **Porter, T., S. L. Pennington, G. M. Adair, R. S. Nairn, and J. H. Wilson.** 1990. A novel system for recombinational and mutational events within an intron of a eucaryotic gene. Nucleic Acids Res. **18:**5173–5180.
24. **Puchta, H., B. Dujon, and B. Hohn.** 1993. Homologous recombination in plant cells is enhanced by in vivo induction of double strand breaks into DNA by a site-specific endonuclease. Nucleic Acids Res. **21:**5034–5040.
25. **Roth, D. B., X. B. Chang, and J. H. Wilson.** 1989. Comparison of filler DNA at immune, nonimmune, and oncogenic rearrangements suggests multiple mechanisms of formation. Mol. Cell. Biol. **9:**3049–3057.
26. **Roth, D. B., and J. H. Wilson.** 1985. Relative rates of homologous and nonhomologous recombination in transfected DNA. Proc. Natl. Acad. Sci. USA **82:**3355–3359.
27. **Roth, D. B., and J. H. Wilson.** 1988. Illegitimate recombination in mammalian cells, p. 621–653. *In* R. Kucherlapati and G. R. Smith (ed.), Genetic recombination. American Society for Microbiology, Washington, D.C.
28. **Rouet, P., F. Smih, and M. Jasin.** 1994. Expression of a site-specific endonuclease stimulates homologous recombination in mammalian cells. Proc. Natl. Acad. Sci. USA **91:**6064–6068.
29. **Rouet, P., F. Smih, and M. Jasin.** 1994. Introduction of double-strand breaks into the genome of mouse cells by expression of a rare-cutting endonuclease. Mol. Cell. Biol. **14:**8096–8106.
30. **Sargent, R. G., R. V. Merrihew, R. Nairn, G. Adair, M. Meuth, and J. H. Wilson.** 1996. The influence of a GT_{29} microsatellite sequence on homolo-

gous recombination in the hamster adenine phosphoribosyltransferase gene. Nucleic Acids Res. **24:**746–753.
31. **Segal, D. J., and D. Carroll.** 1995. Endonuclease-induced, targeted homologous extrachromosomal recombination in Xenopus oocytes. Proc. Natl. Acad. Sci. USA **92:**806–810.
32. **Strathern, J. N., B. K. Shafer, and C. B. McGill.** 1995. DNA synthesis errors associated with double-strand-break repair. Genetics **140:**965–972.
33. **Sugawara, N., and J. E. Haber.** 1992. Characterization of double-stand break-induced recombination: homology requirements and single-stranded DNA formation. Mol. Cell. Biol. **12:**563–575.
34. **Vanlerberghe, F., F. Bonhomme, C. A. I. Hutchison, and M. H. Edgell.** 1993. A major difference between the divergence patterns within the lines-1 families in mice and voles. Mol. Biol. Evol. **10:**719–731.
35. **Wu, T. C., and M. Lichten.** 1994. Meiosis-induced double-strand break sites determined by yeast chromatin structure. Science **263:**515–518.